06.5;08.1

Effect of Nitrogen Plasma Treatment on the Structural and Optical Properties of InGaN

© V.O. Gridchin[1–3], I.P. Soshnikov[2–4], R.R. Reznik[1], S.D. Komarov[5], E.V. Pirogov[2], V.V. Lendyashova[1,2,4], K.P. Kotlyar[1–3], N.V. Kryzhanovskaya[5], G.E. Cirlin[1–4]

[1] St. Petersburg State University, St. Petersburg, Russia
[2] Alferov Federal State Budgetary Institution of Higher Education and Science Saint Petersburg National Research Academic University of the Russian Academy of Sciences, St. Petersburg, Russia
[3] Institute of Analytical Instrument Making, Russian Academy of Sciences, St. Petersburg, Russia
[4] Ioffe Institute, St. Petersburg, Russia
[5] National Research University Higher School of Economics, St. Petersburg, Russia
E-mail: gridchinvo@gmail.com

Received December 6, 2022
Revised December 26, 2022
Accepted December 27, 2022

The effect of cooling conditions in the plasma-assisted molecular-beam epitaxy growth on the structural and optical properties of InGaN nanostructures is studied. It is shown that cooling of the samples without nitrogen plasma contributes to the suppression of phase separation in InGaN nanostructures. The integrated intensity of photoluminescence from these nanostructures increased by a factor of 2.

Keywords: InGaN, silicon, nanostructures, photoluminescence, structural properties, optical properties, molecular beam epitaxy, nitrogen plasma.

DOI: 10.21883/TPL.2023.03.55679.19452

InGaN-based solid solutions are direct-bandgap semiconductor materials with a bandgap width varying from 0.7 (InN) to 3.43 eV (GaN). In view of this, they are considered promising for application in renewable energy sources (specifically, solar water-splitting devices [1,2]). It is known that the visible and IR ranges constitute up to 80% of the solar spectrum; therefore, solid InGaN solutions containing more than 25% In are of particular interest. However, InGaN with an increased In content has a lower crystalline quality and exhibits phase separation over elemental composition, which is the key factor limiting its applicability [3,4]. The plasma-assisted molecular beam epitaxy (PA-MBE) offers ample potential for growth of high-quality epitaxial InGaN nanostructures. An ultrahigh-vacuum environment renders the precautionary measures against parasitic gas-phase reactions unnecessary. Relatively low operating pressures and the use of high-purity materials (high-purity nitrogen and group III elements (7N)) help minimize the contamination of epitaxial layers. PA-MBE growth processes are far from thermodynamic equilibrium, thus potentially facilitating the growth of InGaN of a fine crystalline quality within the entire range of chemical compositions [5,6]. However, most published studies [7–13] were focused on the influence of fluxes of group III and V elements and the growth temperature on the formation of InGaN nanostructures. In the present study, we examine the effect of post-growth processing in nitrogen plasma on the structural and optical properties of InGaN.

InGaN nanostructures were grown on clean *n*-type Si(111) substrates with a chemically polished working surface. Growth experiments were performed in a Riber Compact 12 setup equipped with an Addon RF-N 600 nitrogen plasma source and molecular sources of Ga, In, Al, Mg, and Si. Prior to growth, the substrate was cleaned thermally in the growth chamber at a temperature of 950°C for 20 min to remove residual silicon oxide. At the next stage, the substrate temperature was reduced to 570°C, and the nitrogen plasma source was ignited. Its power was 450 W. The nitrogen flux was 0.4 sccm, which corresponded to a pressure of $7.4 \cdot 10^{-6}$ Torr in the growth chamber. The sample growth time was 20 h. The beam-equivalent pressures of Ga and In were $0.5 \cdot 10^{-7}$ and $1.5 \cdot 10^{-7}$ Torr, respectively. Series of samples with different parameters of cooling to room temperature after epitaxial growth were prepared. In the first case, cooling was performed with the nitrogen plasma source switched on and In and Ga fluxes cut off (set *A*); in the second case, the nitrogen plasma source was switched off and metal fluxes were cut off (set *B*). The cooling rate was 20°C/min.

Preliminary *in situ* monitoring of the sample surface state in real time was performed using reflected high-energy electron diffraction (RHEED). All the grown InGaN samples featured point reflections corresponding to the wurtzite crystal structure [14] in RHEED patterns. The morphology of samples was examined with a Carl Zeiss AG-Supra 25 scanning electron microscope (SEM). The crystal structure of samples was studied by X-ray diffractometry (DRON-8 with CuK_α radiation). Photoluminescence (PL) spectra of samples were measured at room temperature using a helium–cadmium laser with an operation wavelength of 325 nm at a power of 15.5 mW and a laser spot diameter of 100 μm. The PL signal was recorded with an MS5204i

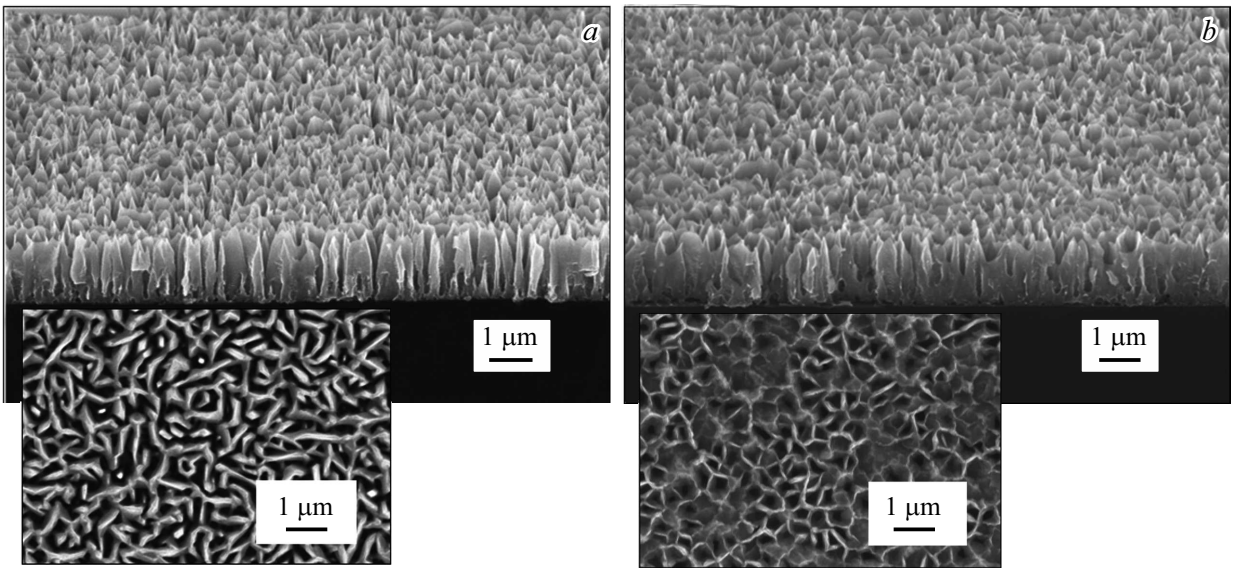

Figure 1. SEM images of InGaN nanostructures. *a* — Samples that were cooled with the nitrogen plasma source switched on (Set A); *b* — Samples that were cooled with the nitrogen plasma source switched off (Set B). Plane-view SEM images of the same series of samples are shown in the insets.

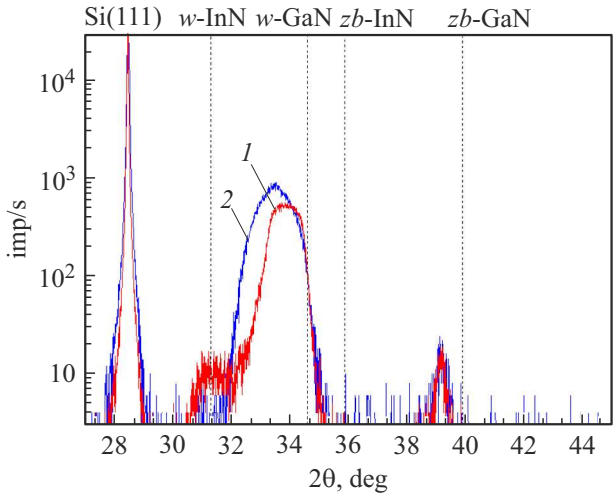

Figure 2. Diffraction patterns of set *A* and *B* samples. Curves *1* and *2* correspond to the measurement data for series *A* and *B* samples, respectively.

monochromator, a single-channel Si detector for the visible range, and an InGaAs lock-in amplifier for the IR range (SRS 510, Stanford Research Systems).

Figure 1 presents the typical SEM images of grown InGaN nanostructures, which have the shape of columns with a height of approximately $1.8\,\mu$m and lateral dimensions of $0.2-0.3\,\mu$m. The upper ends of these columns are pointed. In addition, coalescence of individual columns is observed. Structures of this type are called nanowall networks in literature [2,10,11]. In set *A* samples, individual columns tend to form separate bands with a length of $1-3\,\mu$m. Note that the coalescence (bridging) of columns is observed primarily in the region above $0.5\,\mu$m, while pores are retained below this level. The morphology of series *B* samples is different: they have a network structure with bridging of columns primarily along the projections of $\langle 112 \rangle$ directions. In addition, the formation of film-lamellar lateral coverage of regions with a length up to $5\,\mu$m and a thickness below 50 nm is observed.

Figure 2 presents the $\theta-2\theta$ diffraction curves for grown structures. These curves feature peaks around 27, 31.3, $32-35$, and 39°. The peak near 27° corresponds to the 002 reflection of silicon (substrate material). The peak at 31.3° and the broad $32-35^\circ$ peak are produced by 0002 reflections of InN and $In_xGa_{1-x}N$ solid solutions, respectively. The weak peak in the region of 39° may be associated with the 002 reflection of the cubic phase of InGaN that is produced as multiple stacking faults [15,16]. Comparing the width of InGaN peaks and the sizes of crystallites determined by SEM, we found evidence of dispersion of the chemical composition.

The position of the peak in the $32-35^\circ$ region for series *A* samples corresponds to composition $x \sim 0.25 \pm 0.20$ ($In_xGa_{1-x}N$). The peak at 31.3° is indicative of the presence of the crystalline InN phase. Thus, phase separation over elemental composition is observed in series *A* samples cooled under a flux of chemically active nitrogen.

The curve for series *B* samples has no peak at 31.3°, and the $32-35^\circ$ peak is shifted toward a higher indium content ($x \sim 0.35 \pm 0.20$). This type of diffraction suggests that InGaN structures feature no phase segregation over elemental composition.

Figure 3 shows the PL spectra of the studied samples. IR spectra are presented in the inset. The PL maxima are located near 470 nm. According to the empirical Vegard's

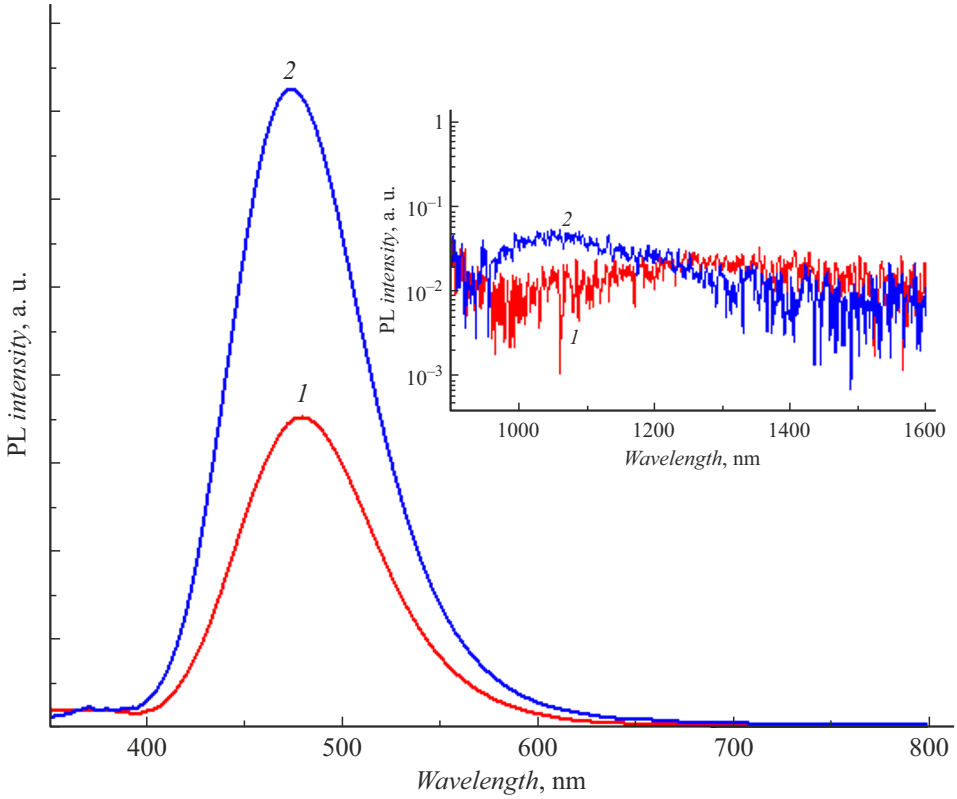

Figure 3. Room-temperature PL spectra of set *A* and *B* samples. Curves *1* and *2* correspond to the measurement data for set *A* and *B* samples, respectively. The PL spectra of samples in the range from 900 to 1600 nm are shown in the inset.

law with bowing parameter $b = 1.43$ eV, this corresponds to In content $x \sim 25\%$ in InGaN. The bandgap energy of InN and GaN were assumed to be equal to 0.7 and 3.43 eV, respectively [17,18]. The integrated PL intensity of series *A* samples is two times lower than the one for series *B* samples. This is apparently attributable to the wurtzite InN phase and defects forming on the InGaN surface under the influence of nitrogen plasma. Room-temperature PL of pure InN was not observed in the 900–1600 nm range. A broad noise-level PL region is likely formed by defects of various types in InGaN.

Thus, the influence of nitrogen plasma on the structural and optical properties of InGaN in the process of cooling to room temperature in the growth chamber was examined. It was demonstrated that the crystalline InN phase may form under these conditions, while the integrated intensity of photoluminescence of InGaN may decrease by a factor of 2. In contrast, the procedure of sample cooling with the nitrogen plasma source switched off and Ga and In sources shut off suppresses phase separation over elemental composition and contributes to an increase in photoluminescence efficiency of InGaN nanostructures.

Funding

Experiments on InGaN nanostructure growth were supported by the Russian Science Foundation (project No. 23-22-00349). The study of structural properties of samples was supported financially by the St. Petersburg State University as part of research grant No. 94031047. PL studies were carried out as part of the Fundamental Research Program of the National Research University Higher School of Economics.

Conflict of interest

The authors declare that they have no conflict of interest.

References

[1] S. Chu, W. Li, Y. Yan, T. Hamann, I. Shih, D. Wang, Z. Mi, Nano Futures, **1** (2), 022001 (2017). DOI: 10.1088/2399-1984/aa88a1
[2] N.H. Alvi, P.E.D. Soto Rodriguez, P. Kumar, V.J. Gómez, P. Aseev, A.H. Alvi, M.A. Alvi, M. Willander, R. Nötzel, Appl. Phys. Lett., **104** (22), 223104 (2014). DOI: 10.1063/1.4909515
[3] I. Ho, G. Stringfellow, Appl. Phys. Lett., **69** (18), 2701 (1996). DOI: 10.1063/1.117683
[4] M.A. Der Maur, A. Pecchia, G. Penazzi, R. Walter, D.C. Aldo, Phys. Rev. Lett., **116** (2), 027401 (2016). DOI: 10.1103/PhysRevLett.116.027401
[5] K.F. Jorgensen, B. Bonef, J.S. Speck, J. Cryst. Growth, **546**, 125738 (2020). DOI: 10.1016/j.jcrysgro.2020.125738

[6] H. Turski, M. Siekacz, Z.R. Wasilewski, M. Sawicka, S. Porowski, C. Skierbiszewski, J. Cryst. Growth, **367**, 115 (2013). DOI: 10.1016/j.jcrysgro.2012.12.026
[7] V.O. Gridchin, R.R. Reznik, K.P. Kotlyar, A.S. Dragunova, N.V. Kryzhanovskaya, A.Yu. Serov, S.A. Kukushkin, G.E. Cirlin, Pis'ma Zh. Tekh. Fiz., **47** (21), 32 (2021) (in Russian). DOI: 10.21883/PJTF.2021.21.51626.18894
[8] T. Tabata, J. Paek, Y. Honda, M. Yamaguchi, H. Amano, Phys. Status Solidi C, **9** (3-4), 646 (2012). DOI: 10.1002/pssc.201100446
[9] V.O. Gridchin, K.P. Kotlyar, R.R. Reznik, A.S. Dragunova, N.V. Kryzhanovskaya, V.V. Lendyashova, D.A. Kirilenko, I.P. Soshnikov, D.S. Shevchuk, G.E. Cirlin, Nanotechnology, **32** (33), 335604 (2021). DOI: 10.1088/1361-6528/ac0027
[10] P.E.D. Soto Rodriguez, P. Kumar, V.J. Gómez, N.H. Alvi, J.M. Mánuel, F.M. Morales, J.J. Jiménez, R. García, E. Calleja, R. Nötzel, Appl. Phys. Lett., **102** (17), 173105 (2013). DOI: 10.1063/1.4803017
[11] P. Kumar, P.E.D. Rodriguez, V.J. Gómez, N.H. Alvi, E. Calleja, R. Nötzel, Appl. Phys. Express, **6** (3), 035501 (2013). DOI: 10.7567/APEX.6.035501
[12] S.Valdueza-Felip, E. Bellet-Amalric, A. Núñez-Cascajero, Y. Wang, M.-P. Chauvat, P. Ruterana, S. Pouget, K. Lorenz, E. Alves, E. Monroy, J. Appl. Phys., **116** (23), 233504 (2014). DOI: 10.1063/1.4903944
[13] R.R. Reznik, V.O. Gridchin, K.P. Kotlyar, N.V. Kryzhanovskaya, S.V. Morozov, G.E. Cirlin, Semiconductors, **54** (9), 1075 (2020). DOI: 10.1134/S1063782620090237.
[14] I.P. Soshnikov, G.E. Cirlin, A.A. Tonkikh, V.N. Nevedomskiĭ, Yu.B. Samsonenko, V.M. Ustinov, Phys. Solid State, **49** (8), 1440 (2007). DOI: 10.1134/S1063783407080069.
[15] C.-C. Chen, C.-C. Yeh, C.-H. Chen, M.-Y. Yu, H.-L. Liu, J.-J. Wu, K.-H. Chen, L.-C. Chen, J.-Y. Peng, Y.-F. Chen, J. Am. Chem. Soc., **123** (12), 2791 (2001). DOI: 10.1021/ja0040518
[16] X.M. Cai, Y.H. Leung, K.Y. Cheung, K.H. Tam, A.B. Djurišić, M.H. Xie, H.Y. Chen, S. Gwo, Nanotechnology, **17** (9), 2330 (2006). DOI: 10.1088/0957-4484/17/9/042
[17] G. Orsal, Y.E. Gmili, N. Fressengeas, J. Streque, R. Djerboub, T. Moudakir, S. Sundaram, A. Ougazzaden, J.P. Salvestrini, Opt. Mater. Express, **4** (5), 1030 (2014). DOI: 10.1364/OME.4.001030
[18] V.Yu. Davydov, A.A. Klochikhin, Semiconductors, **38** (8), 861 (2004). DOI: 10.1134/1.1787109.